HHS Public Access

Author manuscript

Mol Cell Biochem. Author manuscript; available in PMC 2017 November 01.

Published in final edited form as:

Mol Cell Biochem. 2015 December ; 410(1-2): 293–300. doi:10.1007/s11010-015-2562-4.

Enhanced Anti-fibrogenic Effects of Novel Oridonin Derivative CYD0692 in Hepatic Stellate Cells

Fredrick J. Bohanon, MD[a,e], **Xiaofu Wang, BS**[a], **Brittany M. Graham, MD**[a,f], **Anesh Prasai, BS**[d,e], **Sadhashiva J. Vasudevan, BS**[a], **Chunyong Ding, PhD**[b], **Ye Ding, PhD**[b], **Geetha L. Radhakrishnan, MD**[c], **Cristiana Rastellini, MD**[a], **Jia Zhou, PhD**[b,*], and **Ravi S. Radhakrishnan, MD**[a,c,*]

[a]Department of Surgery, University of Texas Medical Branch, 301 University Blvd., Galveston, TX, 77555, USA

[c]Department of Pediatrics, University of Texas Medical Branch, 301 University Blvd., Galveston, TX, 77555, USA

[b]Chemical Biology Program, Department of Pharmacology and Toxicology, University of Texas Medical Branch, 301 University Blvd., Galveston, TX, 77555, USA

[d]Department of Cell Biology and Neuroscience, University of Texas Medical Branch, 301 University Blvd., Galveston, TX, 77555, USA

[e]Shriners Hospital for Children-Galveston, 815 Market St. Galveston, TX 77550, USA

[f]School of Medicine, University of Texas Medical Branch, 301 University Blvd., Galveston, TX, 77555, USA

Abstract

Aim—Oridonin, isolated from *Rabdosia rubescens*, has been proven to possess various anti-neoplastic and anti-inflammatory properties. Previously, we reported the anti-fibrogenic effects of oridonin for liver *in vitro*. In the present study, we investigated the effects of a newly designed analogue CYD0692 *in vitro*.

Methods—Cell viability was measured by Alamar Blue assay. Cell apoptosis was assessed by Cell Death ELISA and Yo-Pro-1 staining. Western Blots were performed for cellular proteins. Flow Cytometry was used to measure cell cycle regulation.

Results—CYD0692 significantly inhibited LX-2 cells proliferation in a dose- and time-dependent manner with an IC_{50} value of ~0.7 μM for 48 hours, ~10 –fold greater potency than oridonin. Similar results were observed in HSC-T6 cells. In contrast, on the human hepatocyte cell line C3A, only 12% of the cell growth was inhibited with 5 μM of CYD0692 treatment for 48h, while 30% inhibited at 10 μM. After CYD0692 treatment on LX-2 cells, apoptosis and S-phase cell cycle arrest were induced; cleaved-PARP, p21, and p53 were activated while cyclin-B1 levels

Send correspondence to: Ravi S. Radhakrishnan, Department of Surgery, The University of Texas Medical Branch, 301 University Boulevard, Galveston, Texas 77555-0353, Telephone: (409) 772-5666, FAX: (409) 772-4253, rsradhak@utmb.edu. Co-corresponding author: Jia Zhou, Chemical Biology Program, Department of Pharmacology and Toxicology, University of Texas Medical Branch, Galveston, Texas 77555-0353, United States, Tel: (409) 772-9748; Fax: (409) 772-9648; jizhou@utmb.edu.

Presented as a poster at the Digestive Disease Week meeting in Chicago, IL May 3–6, 2014.

declined. In addition, α-smooth muscle actin, type I Collagen, and fibronectin (FN) were markedly down regulated. Transforming growth factor β1 (TGF β1) has been identified as a dominant stimulator for ECM production in HSC. Our results indicated that pre-treatment with CYD0692 blocked TGF β1-induced FN expression, thereby decreasing the downstream factors of TGF β1 signaling, such as Phospho-Smad2/3 and phospho-ERK.

Conclusion—In comparison with oridonin, its novel derivative CYD0692 has demonstrated to be a more potent and potentially safer anti-fibrogenic agent for the treatment of hepatic fibrosis.

Keywords

Oridonin; liver fibrosis; stellate cells; apoptosis; ECM

INTRODUCTION

Persistent liver injury results in chronic liver disease (CLD) due to unrelenting activation of the fibrotic pathway. Worldwide viral hepatitis is the leading cause of CLD followed by toxin induced (e.g. alcohol), altered metabolic condition, and autoimmune etiologies. Uncorrected fibrosis is considered as the driving force leading to cirrhosis. Thirty-one million disability-adjusted life years (DALYs) and 2% of all deaths were due to liver cirrhosis in 2010 [1]. Liver fibrosis, if left untreated, leads to cirrhosis that is part of a dynamic wound healing process with phases of extracellular matrix (ECM) protein deposition and degradation [2, 3]. When there is a net positive deposition of ECM, liver fibrosis progresses.

Activated Hepatic stellate cells (HSC) are the major source of ECM proteins within the liver [2]. Quiescent HSC reside within the space of Disse and comprise 2–10% of the cell population [4]. Quiescent HSC become activated HSC following a variety of stimuli such as transforming growth factor β1 (TGF β1), lipopolysaccharide (LPS)/toll-like receptors, tissue hypoxia, platelet-derived growth factors (PDGF), nicotinamide adenine dinucleotide phosphate-oxidase (NADPH), and the renin-angiotensin system [5, 6]. This activation is characterized by over expression of α-smooth muscle actin (α-SMA), excessive production of collagen Type I and III, chemokines, adhesion molecules and presentation of antigens to T cells and Natural Killer (NK) cells [7–10].

Currently available treatment is focused on elimination of the etiological agent, but alleviation of HSC activation may supplement therapy [11]. We have previously reported that oridonin, an active compound isolated from *Rabdosia rubescens*, inhibits HSC proliferation and fibrogenesis [12]. Oridonin has demonstrated the ability to decrease HSC cell viability, increase apoptosis, and decrease both endogenous and TGF β1 stimulated ECM production by HSCs. While oridonin has been extensively studied in cancer treatment, previous work from our team indicated that design and development of novel oridonin analogues could generate more potent and safer compounds with better drug properties [13–16].

In the present study, we propose that CYD0692, a newly designed oridonin analogue, exhibits more potent anti-fibrogenic effects by inhibiting HSC activation, proliferation and ECM production in an *in vitro* model.

METHODS

Reagents

All cell culture mediums and trypsin were purchased from Life Technology Corp. (Carlsbad, CA). Oridonin and antibody against α-smooth muscle actin (α-SMA) (Cat#5228) were purchased from Sigma-Aldrich Co. LLC. (St. Louis, MO). Transforming growth factor β1 (TGFβ1) was purchased from R&D Systems Inc. (Minneapolis, MN). Propidium iodide was purchased from MP Biomedicals, LLC (Solon, OH). Antibodies against Fibronectin (sc-6952) were purchased from Santa Cruz Biotechnology Inc. (Santa Cruz, CA). Anti-Collagen Type I polyclonal antibody (600-401-103) was purchased from Rockland Immunochemicals Inc. (Gilbertsville, PA). GAPDH antibody (10R-G109A) was purchased from Fitzgerald Industries (Concord, MA). Anti-p21 (Cat#556431) was purchased from BD Biosciences (San Jose, CA). Anti-p53 (Cat#2527), phospho-p53 (Cat#9286), cleaved PARP (Cat#5625), cleaved caspase-9 (Cat#9505), phospho-ERK 1/2 (Cat#4377) and phospho-Smad 2/3 (Cat#8828) were purchased from Cell Signaling Technology Inc. (Danvers, MA). Cleaved caspase-3 (ab136812) was purchased from Abcam plc. (Cambridge, MA).

CYD0692 is a novel analogue designed with an additional α-formylenone motif formed in the A-ring and an acetonide moiety introduced at 7,14-dihydroxyl of oridonin (Figure 1). CYD0692 was synthesized following our previously reported protocols [13].

Cell culture

The human immortalized HSC line LX-2 and rat immortalized HSC line HSC-T6 were obtained from Dr. Scott Friedman (Mount Sinai Medical Center, New York) and cultured at 37° C with 5% CO_2 in Dulbecco's modified Eagle's medium (DMEM) with a high glucose concentration (4.5 g/L) supplemented with 5% fetal bovine serum (FBS), 1% penicillin/streptomycin. Human hepatocyte cell line C3A was obtained from American Type Cell Culture (ATCC, Manassas, VA), and maintained in DMEM medium containing 10% FBS. All experiments were performed on cells within 6 weeks of culture from liquid nitrogen.

Western immunoblotting

Whole cell extracts were prepared as previously described [12]. Briefly, extracts were prepared using RIPA buffer (Thermo Fischer Scientific, Inc., Waltham, MA) with 1% Halt protease inhibitor cocktail and 1% Halt phosphatase inhibitor cocktails (Thermo Fischer Scientific, Inc., Waltham, MA). The protein concentration was measured and quantified by the Bradford method [17]. 10–30 μg of protein was fractionated by sodium dodecyl sulfate-polyacrylamide gel electrophoresis (SDS-PAGE) (Life Technologies Corporation, Grand Island, NY) under denaturing conditions and then electro-transferred to a polyvinylidene fluoride (PVDF) membrane. After being blocked with Blocking buffer (LI-COR, Inc., Lincoln, NE) the membrane was probed with the indicated primary antibody (Ab) diluted with blocking buffer. Membranes were washed three times with Phosphate buffered saline

with 0.1% Tween 20 (PBST), and incubated 1 hour with IRDye 680-conjugated anti-mouse μ or IRDye 800-conjugated anti-rabbit Ab (LI-COR, Inc., Lincoln, NE). Finally, the membranes were washed three times with PBST, and signals were scanned and visualized by Odyssey Infrared Imaging System (LI-COR, Inc., Lincoln, NE).

Cell death detection ELISA assay

8×10^3 cells/well were seeded into 96-well plates. After reaching 70–80% confluence, cells were replaced with fresh complete medium and treated as indicated. Apoptosis was determined using a Cell Death Detection ELISA Kit (product # 11 774 425 001, Roche Diagnostics Corp. Indianapolis, IN) following manufacturer's protocol. Assay was performed in duplicate and repeated twice.

Detection of Yo-Pro-1 uptake

For the detection of apoptosis by Yo-Pro-1 (Life Technologies Corporation, Grand Island, NY), cells were seeded in 24-well plates with 0.25×10^5 cells/well. Next day, cells were treated with 0.75 μM of CYD0692 for 12 hours. After being washed with PBS, cells were incubated with 1 μM of Yo-Pro-1 for 1 hour. Yo-Pro-1 uptake was determined by confocal microscope (Nikon Instruments Inc. Melville, NY).

Alamar blue/cell viability assay

3×10^3cells/well of LX-2 cells, 4×10^3 cells/well of HSC-T6 cells, or 5×10^3 cells/well of C3A cells in 100 μL of complete medium were seeded into 96-well plates. Next day, cells reached 50–60% confluence and were replaced with fresh complete medium and treated as indicated for 24, 48, or 72 hours. Alamar blue stock solution (Life Technologies Corporation, Grand Island, NY) was diluted to 1:1 with culture medium and a volume of 25 μL/well was transferred into the assay plate for final concentration of 10% alamar blue. The plate was returned to the incubator for an additional 4 hours. Fluorescence intensity was monitored using a SpectraMax M2 microplate reader (Molecular Devices, LLC, Sunnyvale, CA) with excitation and emission wavelengths set at 540 and 590 nm, respectively. Assay was performed in triplicate and repeated at least three times.

Cell cycle analysis by flow cytometry

Nuclear DNA content was measured by using propidium iodide staining and fluorescence-activated cell sorter analysis. Briefly, 2×10^6 adherent cells were trypsinized, washed with phosphate-buffered saline, resuspended in a low-salt stain solution (3% polyethylene glycol 8000, 50 μg of propidium iodide per mL, 0.1% Triton X-100, 4 mM sodium citrate, 180 units of RNase A per mL), and incubated at 37°C for 20 minutes. An equal volume of high-salt stain solution (3% polyethylene glycol 8000, 50 μg of propidium iodide per ml, 0.1% Triton X-100, and 400 mM sodium chloride) was then added to the cell suspension. Propidium iodide-stained nuclei were stored at 4°C at least 3 hours before fluorescence-activated cell sorter analysis using BD FACSCanto II flow cytometer (Becton, Dickinson and Company, Franklin Lakes, NJ) at the University of Texas Medical Branch Flow Cytometry and Cell Sorting Core Facility. ModFit LT for Win32 software was used for data analysis (Verity Software House, Inc., Topsham, ME).

Statistical analysis

Statistical analysis was performed using GraphPad 6.0 (GraphPad Prism, GraphPad Software Inc. La Jolla, CA) were used. All summary bar and line graphs are presented as mean ± standard error of the mean (SEM), with significance defined as $p < 0.05$.

Results

CYD0692 inhibits HSC proliferation more potently than oridonin

Chemical structure of CYD0692 as compared to oridonin is shown in Figure 1. HSC proliferation and activation are determinants of its fibrogenic potential. To explore the antifibrotic effects of CYD0692 in comparison with oridonin, Alamar Blue assay was used to assess the viability of LX-2 cells after CYD0692 and oridonin treatment, respectively. As shown in Figure 2A, CYD0692 significantly reduced LX-2 cell viability in a dose-dependent manner. Importantly, CYD0692 was significantly more potent with a calculated IC_{50} value of 0.70 μM compared to that of oridonin (*i.e.* 7.5 μM). Figure 2B demonstrates that CYD0692 significantly decreased LX-2 cell viability at 24, 48, and 72 hours as compared to the control. To further confirm these findings, the anti-proliferative effect of CYD0692 was significantly more potent (Figure 2C) than oridonin in the rat hepatic stellate cell line HSC-T6. Next, C3A cells were used to assess the cytotoxic effects of CYD0692 on human hepatocytes. C3A, a clonal derivative of HepG2 cells, were used for their more normal hepatocyte phenotype [18, 19]. Illustrated in Figure 2D, CYD0692 had no significant impact on cell viability over a range of concentrations, being comparable to oridonin. In summary, CYD0692 significantly attenuated activated hepatic stellate cell viability without cytotoxic effects on hepatocytes.

CYD0692 induces LX-2 cell cycle arrest

To examine the anti-proliferative mechanism of CYD0692, cell cycle progression in LX-2 cells was determined using flow cytometry. CYD0692 treatment at 24 hours resulted in a significant increase in S-phase arrest compared to the 0.1% DMSO control (Figure 3A; 30.12 ± 0.34 vs. 35.89 ± 0.77, $p = 0.02$). Since the majority of cells were in G_0–G_1 phase under normal conditions, we did not synchronize cells before flow cytometry.

Next, we assessed the effect of CYD0692 on cell cycle regulatory proteins through Western Blot analyses (Figures 3B and 3C). CYD0692 treatment resulted in a significant increase in phosphorylated-p53, while no change in total p53 was observed. Further, there was a significant decrease in Cyclin B1 expression at 8 hours, which continued throughout the study period. In addition, p21 levels were significantly increased at 8–24 hours. CYD0692 had no significant effect on C3A cell proliferation at our target dose (0.75 μM). To examine the possible mechanism of this effect, immunoblot assay was performed to assess the expression of p53 and p21. CYD0692 had no significant effect on p53 or p21 expression levels (Figure 3D).

CYD0692 promotes LX-2 cell apoptosis

Using the Cell Death Detection ELISA, LX-2 cell apoptosis was evaluated to determine whether apoptosis was involved in decreased HSC viability. The Cell Death Detection

ELISA measures the cytosolic histone fragments, which are a hallmark of apoptosis [20]. CYD0692 treatment resulted in a significant increase in apoptosis at 48 hours (Figure 4A). This was confirmed with Yo-Pro-1 staining, which detects early apoptosis [21]. Figure 4B demonstrates that vehicle-treated cells were negative for Yo-Pro-1 staining, while CYD0692 treated cells stained positive at 24 hours, indicating early apoptosis. Using Western Blot analyses, cleaved caspase-3 and cleaved-PARP levels were found to be significantly increased at 24 hours post-treatment (Figure 4C). However, CYD0692 had no significant effect on caspase-9 (data not shown).

CYD0692 suppresses endogenous and TGF-β induced extracellular matrix protein expression

The activated HSC is a central player in the development of fibrosis. A hallmark of HSC activation is over expression of α-SMA and increased production of Type I Collagen and fibronectin. The effects of CYD0692 on endogenous α-SMA and ECM production were assessed by Western Blot analysis. LX-2 cells were treated with CYD0692 for 24, 48 and 72 hours and total cellular protein was isolated for analysis. CYD0692 decreased α-SMA expression at 48 and 72 hours (Figure 5A). Fibronectin and Type I Collagen expression were significantly decreased at all-time points (Figure 5B). MMP-3, an ECM degradation protein, had significantly elevated expression at 4, 8, 12 and 16 hours after treatment with CYD0692 (Figure 5C). TGF-β is one of the most potent stimulators of ECM production in hepatic fibrosis [22]. We examined the effects of CYD0692 on the TGF-β signaling cascade and TGF-β induced ECM protein production. As shown in Figure 5D, TGF-β treatment significantly increased the production of phosphorylated-Smad 2/3, phosphorylated-ERK 1/2 and fibronectin. Two hour pretreatment with CYD0692 significantly inhibited the production of phosphorylated-Smad 2/3 and fibronectin and reduced the expression of phosphorylated-ERK 1/2 to basal levels.

Discussion

We have previously reported that oridonin is capable of inhibiting HSC proliferation, inducing S-phase cell cycle arrest, enhancing HSC apoptosis, attenuating endogenous ECM protein production and blocking TGF-β stimulated ECM protein production [12]. CYD0692, a newly designed analog of oridonin, has been identified to be about 10-fold more potent than oridonin with an IC_{50} value of 0.70 μM, while having minimal effect on C3A cell viability. CYD0692 caused a significant increase in S-phase cell cycle arrest and demonstrated elevated phospho-p53 and p21 levels with decreased cyclin B1. Additionally, CYD0692 caused a significant increase in LX-2 cell apoptosis in a caspase-3 dependent mechanism. We found that CYD0692 mitigated endogenous production of α-SMA and ECM proteins type I collagen and fibronectin as well as inhibited the downstream signaling of the TGF-β pathway with decreased levels of pSmad 2/3, pERK 1/2, and fibronectin.

S-phase arrest is initiated when DNA synthesis is incomplete and p53 is a major player in this checkpoint [23]. For cells progressing to mitosis Cdc2 must bind cyclin B1 and activate Cdc25, and this pathway is inhibited by activation of p53 and the subsequent increase in p21. p21 directly inhibits Cdc2 and p53 represses cyclin B1, leading to cycle arrest[23, 24].

CYD0692 may inhibit DNA synthesis and prevent the proliferation of HSC by activating p53 and increasing p21 levels, while having no effect on hepatocytes. Notably, from our results, C3A cell treatment with identical concentrations (0.75μM) had no effect on p53 or p21 expression, therefore, C3A cell viability was not affected by CYD0692. This may implicate the important role of the p53/p21 pathway in HSC proliferation. Further, CYD0692 results in an increase in HSC apoptosis as evidenced by histone fragment accumulation and Yo-Pro-1 staining, as well as increased activation of cleaved caspase-3 and cleaved-PARP. This is different from the proposed mechanism for oridonin. Oridonin appears to work through a caspase-3 independent mechanism with increased expression of cleaved caspase-9 and cleaved-PARP [12]. This pathway for oridonin's apoptotic effects has been demonstrated in another study [25].

CYD0692 has the capacity to suppress the expression of α-SMA, type I collagen, and fibronectin production at much lower concentrations when compared to oridonin. This finding provides preliminary evidence that CYD0692 may be a novel more potent agent for reducing hepatic fibrosis than its parent compound, oridonin. TGF-β is a major stimulant of hepatic fibrosis. TGF-β binds its receptor and activates a cascade of proteins, of which, Smad 2/3 is the major effector in the activation of the fibrogenic pathway [26]. The ERK pathway is another downstream signaling cascade triggered by TGF-β binding, where TGF-β binds its receptor and activates Ras, which then phosphorylates ERK 1/2 allowing for phosphorylation of Smad 2/3 [27]. CYD0692 inhibited the phosphorylation of Smad 2/3 and reduced the phosphorylation of ERK 1/2 leading to a decrease in fibronectin production. Furthermore, CYD0692 increased the expression of mmp-3. This could also lead to decreased ECM deposition and a decreased fibrosis. Further study into the anti-fibrogenic effects of CYD0692 is warranted to elucidate its exact mechanism of effect.

Oridonin has been used in East Asian folk medicine for hundreds of years for its anti-bacterial and anti-inflammatory properties. More recently, oridonin has been extensively studied in the cancer literature for its promising effects on cancer biology [13, 28–31]. Unfortunately, there is a paucity of data on the toxicity of oridonin and the few studies that have been published illustrate that oridonin may cause anemia, thrombotic events, and causes immunosuppression. Further, oridonin possess only a moderate potency due to its relative insolubility in water [13, 15, 32], [33]. CYD0692 may offer several advantages over oridonin by being significantly more potent, having better solubility, and possibly less toxic effects.

Conclusion

In conclusion, CYD0692 has demonstrated potent antifibrotic properties *in vitro*, indicating its therapeutic potential as a novel safer anti-fibrogenic agent. Further investigation using an *in vivo* liver fibrosis model, such as carbon tetracholoride (CCL_4) or thioacetamide (TAA), is deemed necessary to validate whether CYD0692 will act as a viable, clinically relevant therapy for hepatic fibrosis.

Acknowledgments

This work was supported by grants P50 CA097007, P30 DA028821, R21 MH093844 (JZ), and T32-GM8256 (FJB) from the National Institutes of Health, Cancer Prevention Research Institute of Texas (CPRIT) award, R. A. Welch Foundation Chemistry and Biology Collaborative Grant (JZ) from the Gulf Coast Consortia, BP Fellows Endowment (AP), Shriner's Hospital for Children (SHC 80100) (AP), Anderson Foundation (AP), and John Sealy Memorial Endowment Fund, and the Center for Addiction Research (JZ) from the University of Texas Medical Branch. We would also like to thank Karen Martin for her generous help in preparing our data for publication. We have no conflicts of interest to disclose.

References

1. Novo E, Cannito S, Paternostro C, Bocca C, Miglietta A, Parola M. Cellular and molecular mechanisms in liver fibrogenesis. Arch Biochem Biophys. 2014; 548:20–37. DOI: 10.1016/j.abb.2014.02.015 [PubMed: 24631571]
2. Zhang Y, Ghazwani M, Li J, Sun M, Stolz DB, He F, Fan J, Xie W, Li S. MiR-29b inhibits collagen maturation in hepatic stellate cells through down-regulating the expression of HSP47 and lysyl oxidase. Biochem Biophys Res Commun. 2014; 446:940–4. DOI: 10.1016/j.bbrc.2014.03.037 [PubMed: 24650661]
3. Benyon RC, Arthur MJ. Extracellular matrix degradation and the role of hepatic stellate cells. Semin Liver Dis. 2001; 21:373–84. DOI: 10.1055/s-2001-17552 [PubMed: 11586466]
4. Asahina K. Hepatic stellate cell progenitor cells. J Gastroenterol Hepatol. 2012; 27(Suppl 2):80–4. DOI: 10.1111/j.1440-1746.2011.07001.x [PubMed: 22320922]
5. Lemoinne S, Cadoret A, El Mourabit H, Thabut D, Housset C. Origins and functions of liver myofibroblasts. Biochim Biophys Acta. 2013; 1832:948–54. DOI: 10.1016/j.bbadis.2013.02.019 [PubMed: 23470555]
6. Tsukamoto H, Zhu NL, Wang J, Asahina K, Machida K. Morphogens and hepatic stellate cell fate regulation in chronic liver disease. J Gastroenterol Hepatol. 2012; 27(Suppl 2):94–8. DOI: 10.1111/j.1440-1746.2011.07022.x [PubMed: 22320925]
7. Liu Y, Wang Z, Kwong SQ, Lui EL, Friedman SL, Li FR, Lam RW, Zhang GC, Zhang H, Ye T. Inhibition of PDGF, TGF-β, and Abl signaling and reduction of liver fibrosis by the small molecule Bcr-Abl tyrosine kinase antagonist Nilotinib. J Hepatol. 2011; 55:612–25. DOI: 10.1016/j.jhep.2010.11.035 [PubMed: 21251937]
8. Lee SH, Seo GS, Park YN, Yoo TM, Sohn DH. Effects and regulation of osteopontin in rat hepatic stellate cells. Biochem Pharmacol. 2004; 68:2367–78. DOI: 10.1016/j.bcp.2004.08.022 [PubMed: 15548383]
9. Ramm GA, Shepherd RW, Hoskins AC, Greco SA, Ney AD, Pereira TN, Bridle KR, Doecke JD, Meikle PJ, Turlin B, Lewindon PJ. Fibrogenesis in pediatric cholestatic liver disease: role of taurocholate and hepatocyte-derived monocyte chemotaxis protein-1 in hepatic stellate cell recruitment. Hepatology. 2009; 49:533–44. DOI: 10.1002/hep.22637 [PubMed: 19115220]
10. Winau F, Hegasy G, Weiskirchen R, Weber S, Cassan C, Sieling PA, Modlin RL, Liblau RS, Gressner AM, Kaufmann SH. Ito cells are liver-resident antigen-presenting cells for activating T cell responses. Immunity. 2007; 26:117–29. DOI: 10.1016/j.immuni.2006.11.011 [PubMed: 17239632]
11. Schuppan D, Kim YO. Evolving therapies for liver fibrosis. J Clin Invest. 2013; 123:1887–901. DOI: 10.1172/JCI66028 [PubMed: 23635787]
12. Bohanon FJ, Wang X, Ding C, Ding Y, Radhakrishnan GL, Rastellini C, Zhou J, Radhakrishnan RS. Oridonin inhibits hepatic stellate cell proliferation and fibrogenesis. J Surg Res. 2014; 190:55–63. DOI: 10.1016/j.jss.2014.03.036 [PubMed: 24742622]
13. Ding C, Zhang Y, Chen H, Yang Z, Wild C, Ye N, Ester CD, Xiong A, White MA, Shen Q, Zhou J. Oridonin Ring A-Based Diverse Constructions of Enone Functionality: Identification of Novel Dienone Analogues Effective for Highly Aggressive Breast Cancer by Inducing Apoptosis. J Med Chem. 2013; 56:8814–8825. DOI: 10.1021/jm401248x [PubMed: 24128046]
14. Ding C, Zhang Y, Chen H, Wild C, Wang T, White MA, Shen Q, Zhou J. Overcoming synthetic challenges of oridonin A-ring structural diversification: regio- and stereoselective installation of

azides and 1,2,3-triazoles at the C-1, C-2, or C-3 position. Org Lett. 2013; 15:3718–21. DOI: 10.1021/ol4015865 [PubMed: 23834026]

15. Ding C, Zhang Y, Chen H, Yang Z, Wild C, Chu L, Liu H, Shen Q, Zhou J. Novel nitrogen-enriched oridonin analogues with thiazole-fused A-ring: protecting group-free synthesis, enhanced anticancer profile, and improved aqueous solubility. J Med Chem. 2013; 56:5048–58. DOI: 10.1021/jm400367n [PubMed: 23746196]
16. Ding C, Wang L, Chen H, Wild C, Ye N, Ding Y, Wang T, White MA, Shen Q, Zhou J. ent-Kaurane-based regio- and stereoselective inverse electron demand hetero-Diels-Alder reactions: synthesis of dihydropyran-fused diterpenoids. Org Biomol Chem. 2014; 12:8442–52. DOI: 10.1039/c4ob01040j [PubMed: 25225052]
17. Bradford MM. A rapid and sensitive method for the quantitation of microgram quantities of protein utilizing the principle of protein-dye binding. Anal Biochem. 1976; 72:248–54. [PubMed: 942051]
18. Kelly JH, Darlington GJ. Modulation of the liver specific phenotype in the human hepatoblastoma line Hep G2. In Vitro Cell Dev Biol. 1989; 25:217–22. [PubMed: 2466032]
19. David B, Dufresne M, Nagel MD, Legallais C. In vitro assessment of encapsulated C3A hepatocytes functions in a fluidized bed bioreactor. Biotechnol Prog. 2004; 20:1204–12. DOI: 10.1021/bp034301z [PubMed: 15296449]
20. Sarkar FH, Li Y. Markers of apoptosis. Methods Mol Med. 2006; 120:147–60. [PubMed: 16491600]
21. Fujisawa S, Romin Y, Barlas A, Petrovic LM, Turkekul M, Fan N, Xu K, Garcia AR, Monette S, Klimstra DS, Erinjeri JP, Solomon SB, Manova-Todorova K, Sofocleous CT. Evaluation of YO-PRO-1 as an early marker of apoptosis following radiofrequency ablation of colon cancer liver metastases. Cytotechnology. 2014; 66:259–73. DOI: 10.1007/s10616-013-9565-3 [PubMed: 24065619]
22. Yoshida K, Matsuzaki K. Differential Regulation of TGF-β/Smad Signaling in Hepatic Stellate Cells between Acute and Chronic Liver Injuries. Front Physiol. 2012; 3:53.doi: 10.3389/fphys.2012.00053 [PubMed: 22457652]
23. Taylor WR, Stark GR. Regulation of the G2/M transition by p53. Oncogene. 2001; 20:1803–15. DOI: 10.1038/sj.onc.1204252 [PubMed: 11313928]
24. Charrier-Savournin FB, Château MT, Gire V, Sedivy J, Piette J, Dulic V. p21-Mediated nuclear retention of cyclin B1-Cdk1 in response to genotoxic stress. Mol Biol Cell. 2004; 15:3965–76. DOI: 10.1091/mbc.E03-12-0871 [PubMed: 15181148]
25. Cui Q, Yu JH, Wu JN, Tashiro S, Onodera S, Minami M, Ikejima T. P53-mediated cell cycle arrest and apoptosis through a caspase-3- independent, but caspase-9-dependent pathway in oridonin-treated MCF-7 human breast cancer cells. Acta Pharmacol Sin. 2007; 28:1057–66. DOI: 10.1111/j.1745-7254.2007.00588.x [PubMed: 17588343]
26. Matsuzaki K. Modulation of TGF-beta signaling during progression of chronic liver diseases. Front Biosci (Landmark Ed). 2009; 14:2923–34. [PubMed: 19273245]
27. Mulder KM. Role of Ras and Mapks in TGFbeta signaling. Cytokine Growth Factor Rev. 2000; 11:23–35. [PubMed: 10708950]
28. Xu W, Sun J, Zhang TT, Ma B, Cui SM, Chen DW, He ZG. Pharmacokinetic behaviors and oral bioavailability of oridonin in rat plasma. Acta Pharmacol Sin. 2006; 27:1642–6. DOI: 10.1111/j.1745-7254.2006.00440.x [PubMed: 17112421]
29. Chen G, Wang K, Yang BY, Tang B, Chen JX, Hua ZC. Synergistic antitumor activity of oridonin and arsenic trioxide on hepatocellular carcinoma cells. Int J Oncol. 2012; 40:139–47. DOI: 10.3892/ijo.2011.1210 [PubMed: 21947421]
30. Zhang CL, Wu LJ, Tashiro S, Onodera S, Ikejima T. Oridonin induces a caspase-independent but mitochondria- and MAPK-dependent cell death in the murine fibrosarcoma cell line L929. Biol Pharm Bull. 2004; 27:1527–31. [PubMed: 15467189]
31. Zhou GB, Kang H, Wang L, Gao L, Liu P, Xie J, Zhang FX, Weng XQ, Shen ZX, Chen J, Gu LJ, Yan M, Zhang DE, Chen SJ, Wang ZY, Chen Z. Oridonin, a diterpenoid extracted from medicinal herbs, targets AML1-ETO fusion protein and shows potent antitumor activity with low adverse effects on t(8;21) leukemia in vitro and in vivo. Blood. 2007; 109:3441–50. DOI: 10.1182/blood-2006-06-032250 [PubMed: 17197433]

32. Li S, Liu Y, Liu T, Zhao L, Zhao J, Feng N. Development and in-vivo assessment of the bioavailability of oridonin solid dispersions by the gas anti-solvent technique. Int J Pharm. 2011; 411:172–7. DOI: 10.1016/j.ijpharm.2011.04.006 [PubMed: 21511016]

33. Tian W, Chen SY. Recent advances in the molecular basis of anti-neoplastic mechanisms of oridonin. Chin J Integr Med. 2013; 19:315–20. DOI: 10.1007/s11655-013-1437-3 [PubMed: 23546635]

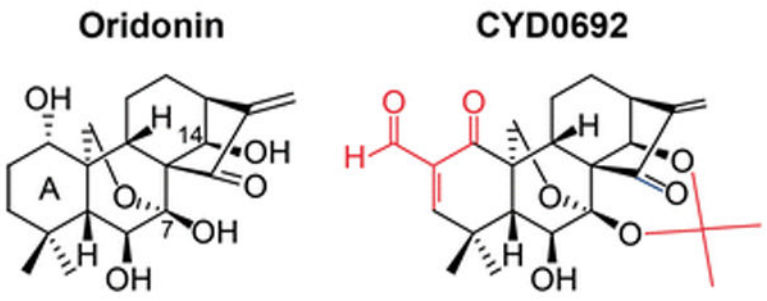

Figure 1.
Chemical structures of oridonin and its new analogue CYD0692.

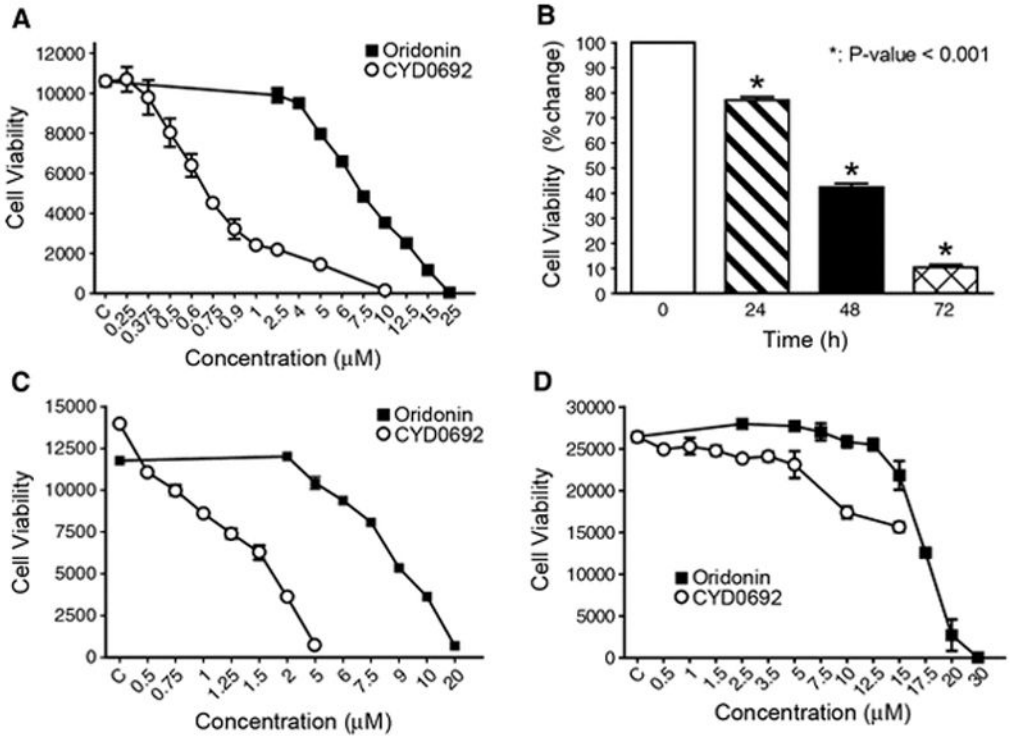

Figure 2.

CYD0692 inhibits HSC proliferation more potently than oridonin. LX-2 cells (A), HSC-T6 cells (C) and C3A hepatocytes (D) were treated with a series of concentrations of CYD0692 for 48 hours, and cell viability was determined using Alamar Blue assay. LX-2 cells were treated with 0.75 μM of CYD0692 for 24, 48, and 72 hours; cell viability was measured by Alamar Blue assay (B). P-values shown compared to vehicle (0.1% DMSO, 0 μM). The results are representative of at least three independent experiments.

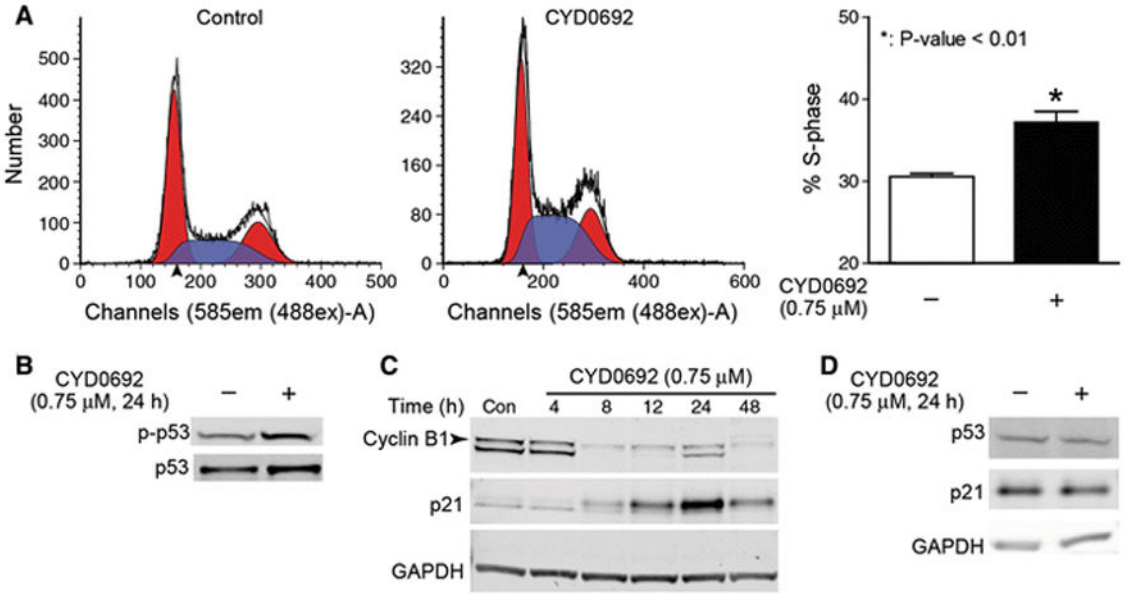

Figure 3.

CYD0692 induces LX-2 cell cycle arrest. CYD0692 induces S-phase cell cycle arrest (A). LX-2 cells were treated with CYD0692 (0.75 μM) for 24 hours. Cells were stained with propidium iodide and analyzed by flow cytometry as described in Methods. (B) and (C) CYD0692 affects cell cycle regulatory proteins. LX-2 cells were treated with vehicle (0.1% DMSO) or CYD0692 (0.75 μM) for indicated time points. Whole cell lysates were analyzed by Western blot with antibodies for p53, p-p53, cyclin B1 and p21. GAPDH was used as loading control. C3A cells were treated with vehicle (0.1% DMSO) or CYD0692 (0.75 μM) for 24 hours. Whole cell lysates were analyzed by Western blot with antibodies for p53 and p21 (D). The experiments were repeated three times and representative data are shown.

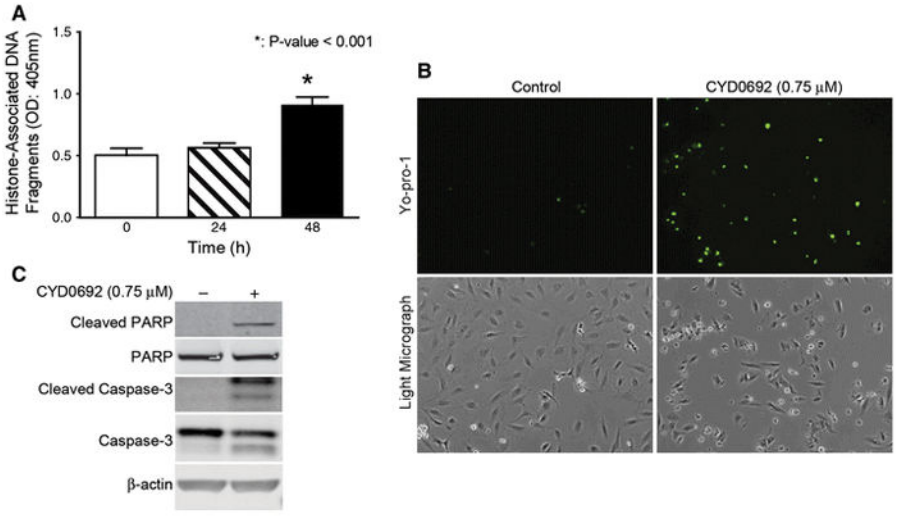

Figure 4.

CYD0692 promotes LX-2 cell apoptosis. LX-2 cells were incubated with CYD0692 (0.75 μM) at indicated time points. Apoptosis by CYD0692 was evaluated either by Cell Death detection ELISA (each conducted in triplicate) (A), or Yo-Pro-1 staining (B). Whole cell lysates were analyzed by Western blot with antibodies for PARP, cleaved-PARP, caspase-3 and cleaved caspase-3 (C). β-actin was used as a loading control. The results are representative of at least three independent experiments.

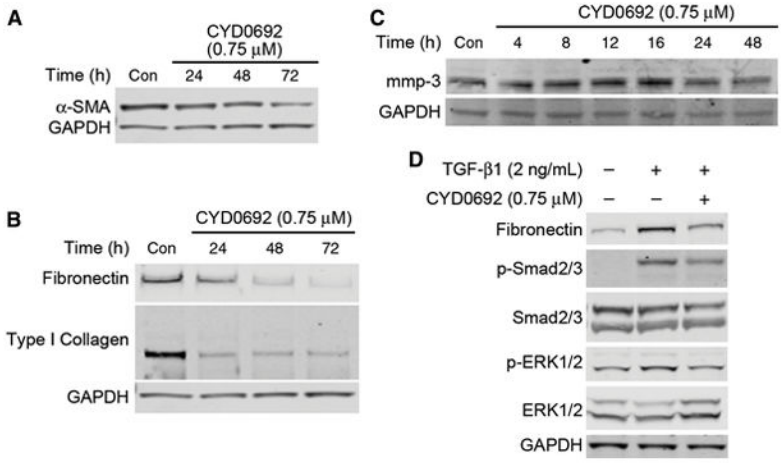

Figure 5.

CYD0692 suppresses endogenous and TGF-β induced ECM protein expression. LX-2 cells were incubated with CYD0692 (0.75 μM) at time points as indicated. Whole cell lysates were analyzed by Western blot with antibodies for α-Smooth muscle actin (A), Type I collagen and fibronectin (B), and mmp-3 (C). LX-2 cells were incubated with CYD0692 (0.75 μM) for 2 hours and then treated with TGF-β (2 ng/mL) for 18 hours (D), whole cell lysates were analyzed by Western blot with antibodies for fibronectin, Smad2/3, phosphorylated-Smad2/3, ERK1/2, and phosphorylated-ERK1/2. GAPDH was used as loading control. The results are representative of at least three independent experiments.